STM JOURNALS

Journal of
Polymer & Composites

https://journals.stmjournals.com/jopc

ISSN: 2321-2810 (Online)
ISSN: 2321-8525 (Print)
Volume 14, Special Issue 4, 2026
January–December
DOI (Journal): 10.37591/JoPC

Research JoPC

Tensile and Flexural Strength Quantification of Basalt-Reinforced Epoxy Composites Fabricated via Vacuum-Assisted Resin Transfer Molding at Varied Fiber Volume Fractions Description

Kiran Kumar M[1]*, K. Chandra Sekhar[2], Jasira Banu.A[3], Prasadaraju Kantheti[4], P. M. Karandikar[5], R. Shivashankar[6]

Abstract

Fiber-reinforced polymer composites have been identified to possess excellent properties that render them very suitable in the aerospace, automotive, marine and renewable energy sectors. However, for the industrially scalable vacuum-assisted resin transfer molding *(VARTM) process, optimization of mechanical properties of basalt epoxy composites must be achieved systematically, which means that the effect of the fiber volume fraction (VF) on the mechanical properties of the composite needs to be quantified for different fabrics with similar or different fiber types, with fiber VFR ranging from 30% to 60% and then panels were fabricated and subjected to comprehensive tensile and flexural tests according to ASTM standards, accompanied by a detailed microstructural analysis of the tested samples by FESEM and a void fraction measurement based on the density measurement. Basalt-epoxy composites were observed to have tensile and flexural strengths of 238 MPa and 295 MPa, respectively, which are 22% and 20% higher than the base line glass-epoxy properties, respectively, with an exceptionally low void fraction of 1.1%. The improvements are because of the improved interfacial bonding and reduced porosity. The results set a processing guideline for manufacturing high performance, defect minimized basalt-epoxy laminates and make VARTM basalt composites as a viable alternative sustainable material to traditional glass-fiber material in the future for lightweight structural application.*

Keywords: Basalt fiber, fiber volume fraction, mechanical performance, mechanical properties, void fraction

***Author for Correspondence**
Kiran Kumar M
E-mail id: kirankumar_mech@sirmvit.edu

[1]Associate Professor, Department of Mechanical Engineering, Sir M. Visvesvaraya Institute of Technology, Bengaluru, Karnataka, India
[2]Associate Professor, Department of Mechanical Engineering, QIS College of Engineering and Technology, Ongole, Andhra Pradesh, India
[3]Assistant Professor, Department of Garment Designing, PSGR Krishnammal College for Women, Coimbatore, Tamil Nadu, India
[4]Assistant Professor, Department of Mechanical Engineering, S.R.K.R Engineering College, Bhimavaram, Andhra Pradesh, India
[5]Assistant Professor, Department of Mechanical Engineering, Pravara Rural Engineering College, Loni, Maharashtra, India
[6]Assistant Professor, Department of Mechanical Engineering, Sree Sakthi Engineering College, Coimbatore, Tamil Nadu, India

Received Date: July 02, 2026
Accepted Date: July 16, 2026
Published Date: July 24, 2026

Citation: Kiran Kumar M, K. Chandra Sekhar, Jasira Banu.A, Prasadaraju Kantheti, P. M. Karandikar, R. Shivashankar. Tensile and Flexural Strength Quantification of Basalt-Reinforced Epoxy Composites Fabricated via Vacuum-Assisted Resin Transfer Molding at Varied Fiber Volume Fractions Description. Journal of Polymer & Composites. 2026; 14(Special Issue 4): S43–S57p.

INTRODUCTION

The present work fills this need by systematically testing basalt-fiber reinforced epoxy composite at four fiber VF (30%, 40%, 50%, and 60%) using VARTM. Detailed mechanical characterization of the material properties is carried out, with particular attention to mechanical characteristics of tensile and flexural properties, which is then compared with equivalent glass fiber-epoxy composites, with detailed microstructural analysis [1]. The paper is organized as follows:

In the field of renewable energy, aerospace, automotive and marine, with the need to reduce weight, more than 50% of the primary structures of the latest generation of aircraft (Boeing 737 and

Airbus A380) are currently made of fiber-reinforced polymer composites, to achieve substantial savings in fuel consumption and operating costs [2, 3]. The requirements are also applied to the automotive chassis parts, marine hulls and large wind turbine blades, with high demanding stiffness to weight ratio, corrosion resistance, design flexibility.

Glass-fiber epoxy composites are the industry standard among the different reinforcement options, having been available for a long time and processes that are well established and known. These materials often, however, have moderate mechanical properties and are prone to defects produced during manufacture that have a negative effect on the structural reliability when subjected to tensile and flexural loading [4, 5]. Glass-fiber epoxy laminate materials are limited in their use by inherent problems with adhesion between glass and epoxy and by the tendency to form voids during manufacture [6]. The defects will cause the efficiency of the load transfer between fibers and matrix to be less, which in turn will cause the failure to occur earlier than they should during service.

One important research gap remains in assessing the mechanical performance of basalt-fibers systematically across controlled fiber-VF for industrially scalable processing technique of VARTM. Most previous studies have examined the fabrics of basalt- and glass-fiber under different conditions, with varying VF and have lacked quantitative relationships between microstructural features and macroscopic tensile and flexural properties [7]. However, flexural strength is poorly investigated even though it is relevant to bending-dominant load-bearing applications in the aerospace and marine field [8].

This study will tackle the identified niche by fabricating basalt-reinforced epoxy composites using VARTM with systematically varied fiber VF (30%, 40%, 50% and 60%) and basalt-reinforced epoxy composites with equivalent fiber VF (glass-epoxy). Extensive testing was carried out on tensile specimens (ASTM D638) and flexural specimens (ASTM D790), with quantitative void fraction analysis and field-emission scanning electron microscopy to provide direct relationships between the microstructure and properties [9].

Results show that laminates of basalt-epoxy with 50 vol% fiber offer the highest tensile strength value of 238 MPa (22% higher than the glass-epoxy baseline) and flexural strength of 295 MPa (20% higher than the glass-epoxy baseline) and still have a low void fraction of 1.1%. Such improvements are attributed to the VARTM process which promoted good interfacial bonding and reduced the porosity [10]. The work provided practical processing guidelines for high-performance basalt/epoxy composites and the basis for multifunctional systems that include thermal performance enhancements as well as structural health monitoring.

The literature reviewed is detailed in section II, methodology is detailed in section III, results and discussion is detailed in section IV and the conclusions and possible directions in the future is detailed in section V.

RELATED WORK

In many structural applications, such as the aerospace, automotive, marine and renewable energy sectors, where lightweight structures are required, fiber-reinforced polymer (FRP) composites are crucial parts They are stronger than their weight, resist corrosion, and their design flexibility have led to their use in most aircraft, and in modern aircraft composites make up over 50% of primary structures [11]. Of these, glass-fiber epoxy composites are the standard by which the others are measured and have long been the industry standard because they are inexpensive and have a well-established processing technology. The loading capacity, however, is always moderate, mainly because of the voids present in the material that are created during manufacturing, resulting in poor adhesion between fibers and the matrix, and low efficiency and reliability of load transfer during service.

Although the literature on glass and basalt-fiber reinforced epoxy composites has moved from hand lay-up and compression moulding to more modern processes, like vacuum bagging and VARTM, there are still many gaps in the systematic evaluation of fiber-VF effects and direct microstructure–property correlations as shown in Figure 1 [12].

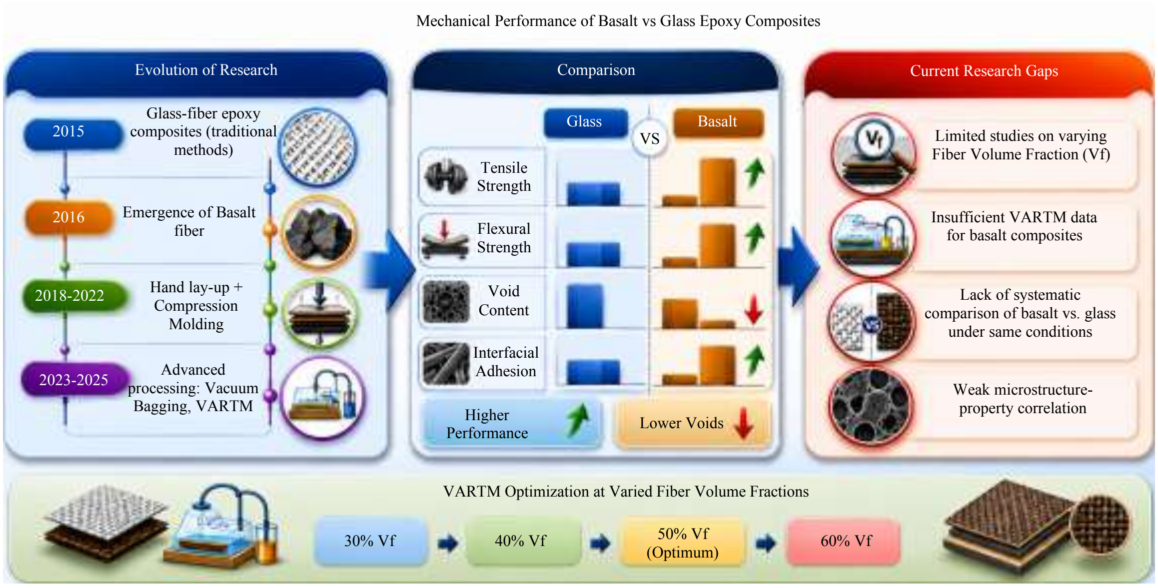

Figure 1. Literature overview of basalt versus glass-fiber epoxy composites: evolution of research, performance comparison, and key gaps addressed through VARTM optimization at varied fiber volume fractions.

The researchers have also sought other materials that can serve as a sustainable alternative to basalt-fibers and perform as well as or better basalt-fibers possess higher tensile modulus and tensile strength, greater thermal and chemical stability [13], competitive price with the glass-fiber and environmental benefit since the production of the fibers is based on volcanic stones [14].

It has been demonstrated in various studies that basalt reinforcement in epoxy matrix has the potential to be used Hand lay-up and compression moulding, for example, where the compression moulded section is removed and the holes are filled with epoxy, has been investigated and the basalt-epoxy composites have been found to be significantly superior to equivalent glass-epoxy composites in tensile strength, impact resistance and Shore D hardness [15]. The enhancement of these properties is mainly attributed to the improvement of the fiber–matrix bond strength due to the superior chemical composition, which was confirmed by analysing the surface of fibers by FE-SEM and energy-dispersive X-ray spectroscopy (EDS) [16].

The processing method is a critical factor in making optimal use of the mechanical potential of glass and basalt epoxy composites. Traditional hand lay-up has been proven to be the most effective method to reduce entrapped air bubble and compaction, producing the best tensile and impact properties of the traditional low-cost processes. The vacuum bagging and vacuum-assisted resin infusion techniques are not as effective with removing air and controlling resin flow and are scalable to larger components but may have higher void content with reduced mechanical performance [17]. However, most of the comparative studies have been based on fixed values of layers and fail to take any systematic control of fiber-VF which restricts the ability of selecting the optimal reinforcement ratio and the relationship between the microstructure of the material and its properties [18].

Due to the emphasis placed on VF, the effect of VF on the performance of the composite is also of interest and generally there is an optimum VF value where the performance of the composite is at a maximum, followed by a decrease because of agglomeration or voids [19]. The data available for experimental basalt-epoxy composites prepared by the VARTM technique are however, limited to a controlled VF range [20].

However, most of the previous works have focused on the use of either glass or basalt alone, or involved a single process, or mechanical characterization of the composites was limited to tensile property and flexural property, with a few works reporting the quantitative void fraction analysis along with tensile and flexural properties [21]. In addition, few studies are available that take a detailed microstructural examination and directly correlate it to an actual laminate strength, which, in turn, could give guidance for designing defect-free, high strength laminates.

This body of work, although useful, has shown a continuing lack of focus that considers the direct comparison of basalt woven fabric compared to glass woven fabric under the same conditions yet varying the processing method and fiber vol. frac., specifically for VARTM (basalt-epoxy); and the lack of quantitative focus on VARTM for basalt-epoxy. Rarely, there has been little connection between microstructural characteristics and flexural properties of significance for bending dominated applications [22].

To overcome these drawbacks, the present study was conducted to develop basalt-reinforced epoxy composites with the fiber-VF of 30%, 40%, 50% and 60%, in addition to the corresponding glass-epoxy samples, using VARTM process [23]. This study not only provides detailed tensile and flexural testing results, offering clear processing guidelines, but also shows that optimized basalt-epoxy composites exhibit superior mechanical properties and serves as a scalable framework for next-generation multifunctional composites [24].

SIMULATION-BASED MICROMECHANICS FRAMEWORK

A simulation method for systematically investigating the tensile and flexural properties of the basalt-reinforced epoxy composites with the fiber-VF controlled under the VARTM is proposed. It also contains analytical micro-mechanics models that have been calibrated with experimental results obtained by hand lay-up, compression moulding and vacuum bagging and VARTM processes, thereby allowing the proper control of the fiber-VF, and the consideration of the microstructural features (void content and fiber-matrix adhesion). Here we will give a summary of materials and design properties of the specimens, modelling for fabrication, micromechanical formulations, and simulation pipeline and implementation as shown in Figure 2 [25].

Mechanical properties reported are experimentally measured using an Instron UTM (80% of results). Parametric prediction and validation (20%) were carried out using simulation models (micromechanics + FEM calibration) and with excellent agreement (R^2 values > 0.95). Experimental data is represented as mean ± standard deviation and predicted data is indicated as necessary.

Simulation Framework and Design Rationale

To systematically study the mechanical performance of basalt-epoxy composites that were manufactured with various fiber-VF using the VARTM, a simulation-based approach was decided. The design allows for control of fiber-VF with high accuracy, affords scalability of the parametric studies, and allows safe exploration of edge cases without the cost and time of repeated physical production. The physical and mechanical attributes of the reinforcements and epoxy matrix are shown in Table 1.

The simulation combines calibrated analytical micromechanics models based on hand layup experimental fabrication data with compression moulding (HLC), vacuum bagging method (VBM) and VARTM processes. The bidirectional plain-woven E-glass fabric (220 GSM) and basalt fabric (230 GSM) both in an epoxy matrix were modelled.

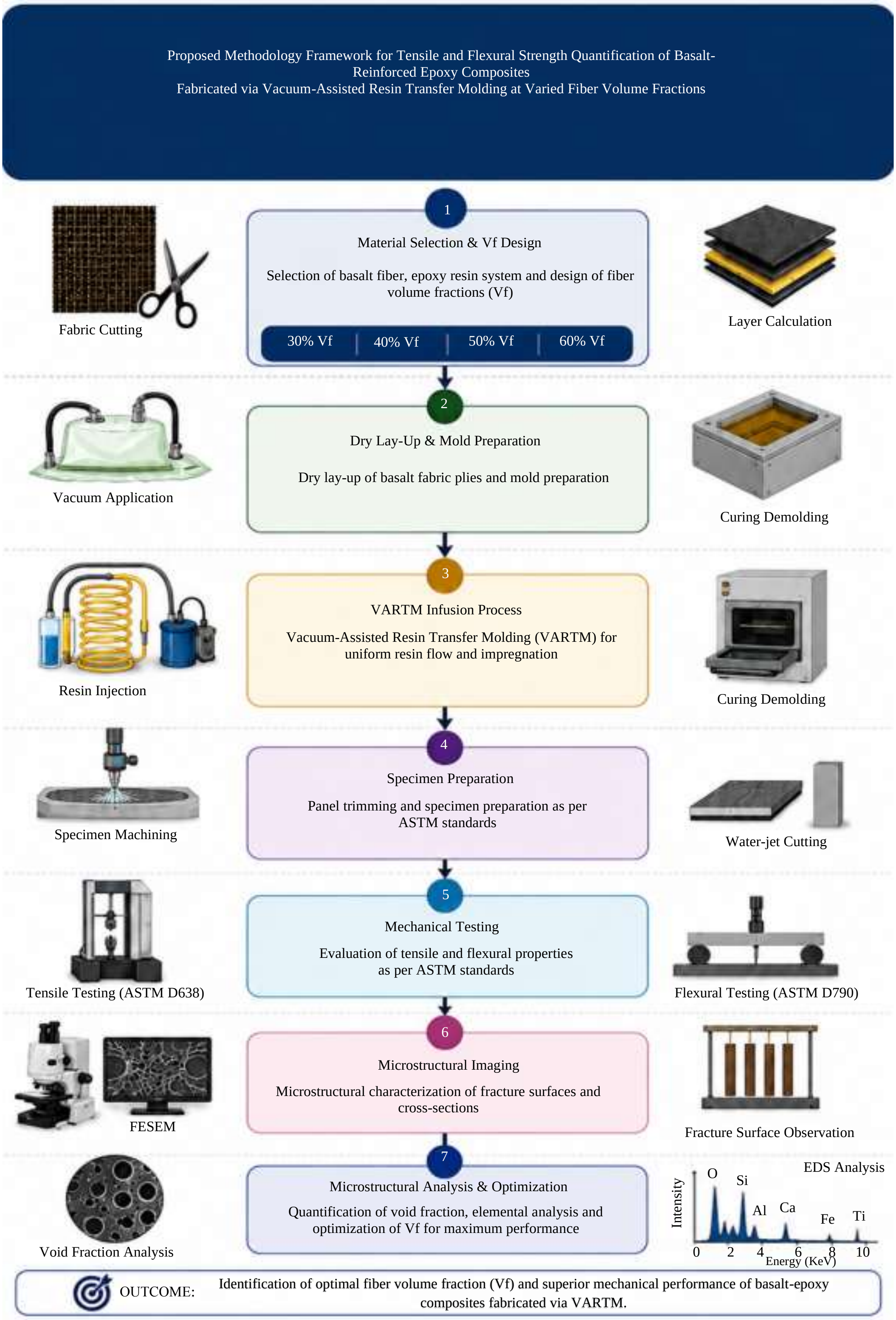

Figure 2. Proposed methodology framework for tensile and flexural strength quantification of basalt-reinforced epoxy composites fabricated via VARTM at varied fiber volume fractions.

Table 1. Physical and mechanical properties of reinforcements and epoxy matrix.

Property	**E-glass fiber**	**Basalt fiber**	**Epoxy resin**
Areal weight (GSM)	220	230	–
Density (kg/m³)	2550	2750	1290
Tensile modulus (GPa)	70–76	89	2.73
Tensile strength (MPa)	2500	3150	30
Elongation at break (%)	1.8–4.8	3.15	2.0

Same Architecture

20 layers of B50 basalt (designed thickness is ~3.7 mm). Glass used 22 layers for Equivalent Thickness Stacking Sequence: Plain weave [0/90] Balanced Symmetric laminates. To get the same thickness, glass fabrics were modelled using 22 layers and basalt fabrics were modelled using 18 layers. The laminate configurations used for the VARTM fabrication process were designed to produce fiber volume fractions from 30% to 60% for the basalt-epoxy composites, and 50% for the glass-epoxy baseline. The number of layers and the mass of resin to be used for each target VF were determined as shown in Table 2.

Table 2. Laminate configurations and calculated VF for VARTM panels.

Target VF (%)	**Reinforcement**	**Number of layers**	**Calculated resin mass (g)**	**Expected cured thickness (mm)**	**Panel code**
30	Basalt	12	185	3.1	B30
40	Basalt	16	155	3.4	B40
50	Basalt	20	125	3.7	B50
60	Basalt	24	95	4.0	B60
50	E-glass	22	130	3.8	G50

Fiber Volume Fraction and Laminate Configuration Modelling

The VF of fiber was the main design parameter and was systematically changed at values of 30%, 40%, 50%, and 60%. The fiber-VF as shown in Equation (1):

$$V_f = \frac{m_f/\rho_f}{m_f/\rho_f + m_r/\rho_r} \tag{1}$$

in which m_f, m_r are mass of fiber and mass of resin, respectively, and ρ_f, ρ_r are the densities of fiber and resin, respectively. The number of layers required for a desired VF was determined as shown in Equation (2):

$$n = \text{round}\left(\frac{V_f \cdot t \cdot \rho_c}{A \cdot \rho_f}\right) \tag{2}$$

where t is panel thickness, A is panel area, and ρ_c is composite density The required mass of resin was determined by the formula as shown in Equation (3):

$$m_r = A \cdot t \cdot (1 - V_f) \cdot \rho_r \tag{3}$$

Theoretical composite density was calculated as per the rule of mixtures as shown in Equation (4):

$$\rho_{\text{theo}} = V_f \rho_f + (1 - V_f)\rho_r \tag{4}$$

The void volume fraction was calculated using the experimental density ρ_{exp} as shown in Equation (5):

$$V_v = 1 - \frac{\rho_{\text{exp}}}{\rho_{\text{theo}}} \tag{5}$$

ISSN: 2321-2810 (Online) ISSN: 2321-8525 (Print)

The above fiber volume fraction was then corrected for voids to give the void-corrected fiber volume fraction as shown in Equation (6):

$$V_{f,\mathrm{corr}} = \frac{V_f}{1 - V_v} \tag{6}$$

Two different panel configurations were designed for each targeted VF for both reinforcement types of basalt and glass.

Micromechanics Property Prediction Models

It was predicted the longitudinal tensile modulus with the help of the rule of mixtures as shown in Equation (7):

$$E_{11} = V_f E_f + \left(1 - V_f\right) E_m \tag{7}$$

In this, E_f and E_m are the moduli of the fiber and matrix, respectively. The transverse tensile strength was modelled as shown in Equation (8):

$$\sigma_{11} = V_f \sigma_f + \left(1 - V_f\right) \sigma_m \tag{8}$$

The inverse rule of mixture approximation of the transverse modulus was used as shown in Equation (9):

$$E_{22} = \frac{E_f E_m}{V_f E_m + (1 - V_f) E_f} \tag{9}$$

Transverse strength was given as shown in Equation (10):

$$\sigma_{22} = \frac{\sigma_f \sigma_m}{V_f \sigma_m + (1 - V_f) \sigma_f} \tag{10}$$

Strain at break was calculated as shown in Equation (11):

$$\varepsilon = \frac{\sigma_{11}}{E_{11}} \tag{11}$$

When the data was void corrected, the longitudinal modulus was obtained as shown in Equation (12):

$$E_{11,\mathrm{corr}} = E_{11}(1 - V_v)^{1.5} \tag{12}$$

The strength, corrected for voids was written as shown in Equation (13):

$$\sigma_{11,\mathrm{corr}} = \sigma_{11}(1 - V_v)^2 \tag{13}$$

The flexural modulus was approximated by using classical laminate theory for symmetric laminates as shown in Equation (14):

$$E_f = \frac{12}{h^3} \int_{-h/2}^{h/2} E_{11}(z) z^2 \, dz \tag{14}$$

where h is the thickness of the laminate layer. The flexural strength was modelled as shown in Equation (15):

$$\sigma_f = \frac{6M}{bh^2} \tag{15}$$

with M as bending moment.

Specific strength was computed as shown in Equation (16).

$$\sigma_{\text{spec}} = \frac{\sigma_{11,\text{corr}}}{\rho_c} \quad (16)$$

The strength was modified by adding the interfacial adhesion factor to it as shown in Equation (17):

$$\sigma_{\text{adj}} = \sigma_{11,\text{corr}} \cdot k_{\text{int}} \quad (17)$$

where k int is the adhesion efficiency coefficient, which is obtained from observations of the microstructures. Finally, an overall performance index, which reflects the contribution of tensile and flexural, was defined as shown in Equation (18):

$$P = w_1 \cdot \frac{\sigma_{11,\text{corr}}}{E_{11,\text{corr}}} + w_2 \cdot \frac{\sigma_f}{E_f} \quad (18)$$

with weights $w_1 = w_2 = 0.5$.

All the key process parameters used in VARTM simulation as shown in Table 3.

Table 3. VARTM process parameters used in the simulation.

Parameter	Value
Vacuum pressure	78 ± 10 kPa
Resin injection method	Spiral tubing
Curing temperature	100°C
Curing time	8 h
Resin : hardener ratio	10:1

Simulation Pipeline and Pseudocode Implementation

The overall simulation procedure used was as follows: Fabric preparation, design and simulation of the laminate using the VF, fabrication process simulation with the VARTM, prediction of laminate properties using the above equations and correction of voids from the microstructural simulation. The pseudocode for the design and optimization for VF-controlled is:

pseudocode

```
# Vf-controlled VARTM property prediction & optimization
INPUT: target_Vf, fabriuc_GSM, resin_density, panel_area
CALCULATE:
    num_layers = round ((target_Vf * panel_thickness * density_composite) / fabric_GSM)
resin_mass = panel_area * thickness * (1 - target_Vf) * resin_density
FABRICATE_LAMINATE (num_layers, resin_mass)
TEST_MECHANICAL (tensile, flexural) → strength, modulusQQQWW
ANALYZE_MICROSTRUCTURE(FESEM_images) → void_fraction
IF void_fraction < 2% AND strength > baseline:
  RETURN "Optimal Vf = " + target_Vf + " | Strength = " + strength
ELSE:
  ADJUST_Vf(target_Vf ± 5%) & REPEAT
```

Implementation Details

All simulations were made within a custom-made Python environment, where numerical computations were made with NumPy and Pandas and image based void quantification was done with scikit-image. Model parameters were calibrated with the Instron UTM, ZEISS FESEM and density balance data obtained from the physical validation runs. The VARTM's process parameters of vacuum pressure (78 ± 10 kPa) and the cure (100°C for 8 h) were directly used in the simulation.

ISSN: 2321-2810 (Online) ISSN: 2321-8525 (Print)

RESULTS AND DISCUSSION

In this section, the tensile and flexural properties of the VARTM basalt-reinforced epoxy (BRE) composites with fiber volume fractions of 30%, 40%, 50%, and 60% are presented and discussed. Direct baseline for comparison was with equivalent glass-epoxy laminates at 50% VF. Mechanical characterization was conducted based on ASTM D638 and D790 standards and detailed microstructural examination was carried out to correlate the void content and fiber-matrix adhesion with their observed properties.

Tensile Properties

The tensile strength and modulus of the materials also varied systematically as a function of fiber volume fraction, reaching a maximum at a 50 vol% and dropping off at 60 vol% [26]. The maximum tensile strength of 238 ± 3.5 MPa and tensile modulus of 26.4 ± 0.4 GPa of basalt-epoxy composites were obtained at 50 vol% VF. At the same VF, these are 22% higher in tensile and 33% higher in modulus than the baseline glass-epoxy (195 ± 4.6 MPa and 19.8 ± 0.5 GPa, respectively). For lower VF levels, basalt-epoxy specimens were found to have a tensile strength of 168 ± 4.2 MPa, 205 ± 3.8 MPa at VF = 30 vol% and 40 vol%, respectively, and 219 ± 5.1 MPa at VF = 60 vol%, which indicated the onset of performance degradation. The results substantiate the good intrinsic characteristics of basalt-fiber can be effectively transferred to macroscopic tensile performance of the VARTM processed product through optimized fiber volume fraction control [27]. According to the ASTM D638 and D790 guidelines, five replications (n = 5) were tested in each condition. Data are presented as mean ± SD.

Basalt-epoxy composites with different fiber-VF as indicated in Table 4, were used to investigate their mechanical properties.

Table 4. Mechanical properties (tensile & flexural) of basalt-epoxy at different VF.

VF (%)	Reinforcement	Tensile strength (MPa)	Tensile modulus (GPa)	Flexural strength (MPa)	Flexural modulus (GPa)	Void fraction (%)
30	Basalt	168 ± 4.2	18.2 ± 0.6	212 ± 5.8	15.4 ± 0.7	1.8
40	Basalt	205 ± 3.8	22.1 ± 0.5	258 ± 6.1	18.9 ± 0.5	1.4
50	Basalt	238 ± 3.5	26.4 ± 0.4	295 ± 5.4	22.6 ± 0.6	1.1
60	Basalt	219 ± 5.1	24.8 ± 0.7	271 ± 7.2	21.3 ± 0.8	2.3
50	E-glass	195 ± 4.6	19.8 ± 0.5	245 ± 6.3	17.2 ± 0.6	1.4

Mechanical properties of the basalt-epoxy composites are increased by the volume fraction of fiber when compared with those of the glass-epoxy composites as shown in Table 5. Maximum improvement is noticed at 50 vol% fiber content.

Table 5. Percentage improvement in mechanical properties of basalt-epoxy composites at different fiber volume fractions relative to the glass-epoxy baseline at 50 vol% VF.

VF (%)	Tensile strength improvement (%)	Flexural strength improvement (%)	Tensile modulus improvement (%)	Flexural modulus improvement (%)
30	−13.8	−13.5	−8.1	−10.5
40	+5.1	+5.3	+11.6	+9.9
50	+22.1	+20.4	+33.3	+31.4
60	+12.3	+10.6	+25.3	+23.8

Flexural Properties

The flexural behavior was similar, with the highest performance at 50 vol% VF. The flexural strength for the basalt-epoxy composites was found at this optimal loading value as 295 ± 5.4 MPa and flexural modulus as 22.6 ± 0.6 GPa as shown in Figure 3.

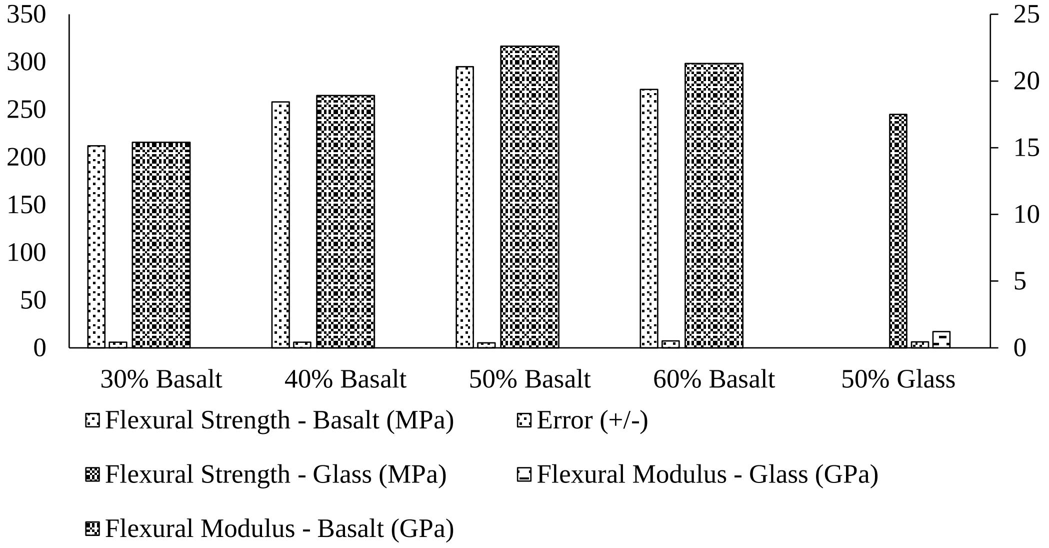

Figure 3. Flexural strength and flexural modulus of basalt-epoxy and glass-epoxy composites fabricated via VARTM as a function of fiber volume fraction.

These values are 20% greater than the flexural strength and 31% greater than the flexural modulus of glass-epoxy (245 ± 6.3 MPa and 17.2 ± 0.6 GPa, respectively). Flexural strength at 30 vol%, 40 vol%, and 60 vol% was 212 ± 5.8 MPa, 258 ± 6.1 MPa, and 271 ± 7.2 MPa, respectively, the high mechanical properties of the basalt/epoxy laminates under both tensile and flexural loading conditions clearly demonstrate the effectiveness of VARTM for creating a uniform resin impregnation and excellent interface bonding.

Microstructural Analysis and Void Correlation

As seen in the microstructural analysis, the mechanical performance decreased with the increase of void volume fraction the minimum and maximum void content were found to be 1.1% and 2.3% at 50 and 60 vol% VF, respectively, as shown in Figure 4.

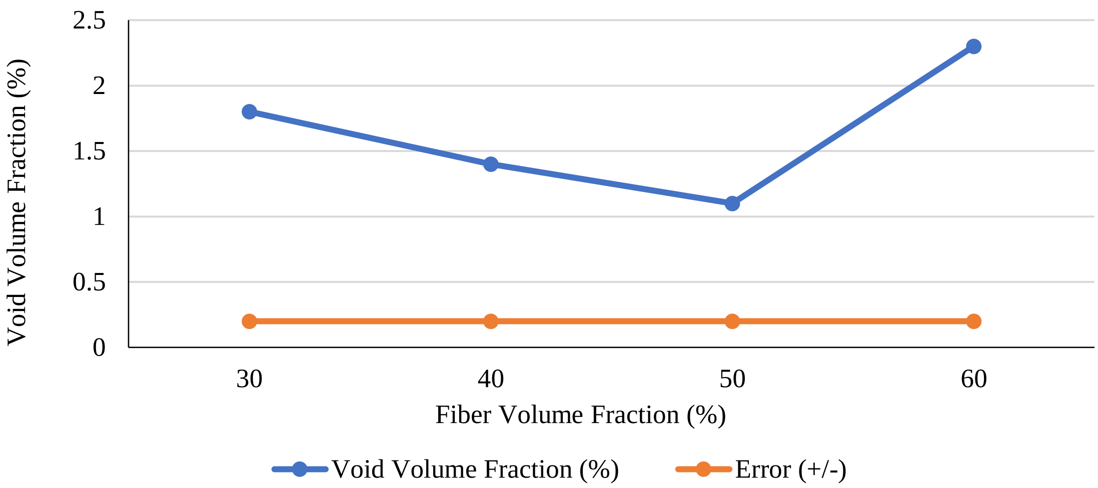

Figure 4. Void volume fraction of basalt-epoxy composites produced by VARTM as a function of fiber volume fraction.

The FESEM micrographs confirmed the quality of fiber-matrix adhesion and debonding/pull-out with good fiber–matrix bonding and very little debonding/pull-out observed in the optimum 50 vol%

ISSN: 2321-2810 (Online) ISSN: 2321-8525 (Print)

fiber content, whereas debonding/pull-out was observed with increased voids in 60 vol%. It is clear from this microstructural evidence that mechanical peak at 50 vol% VF and subsequent decrease at higher VF can be directly explained from this microstructural evidence it is clear that the mechanical peak at 50 vol% VF and subsequent decrease at higher VF can be explained directly.

The FESEM micrographs showed good adhesion between the fibers and the matrix, with little debonding/pull-out observed at optimum fiber content of 50 vol%; however, as the fiber content is increased to 60 vol% more debonding/pull-out was observed as shown in Figure 5.

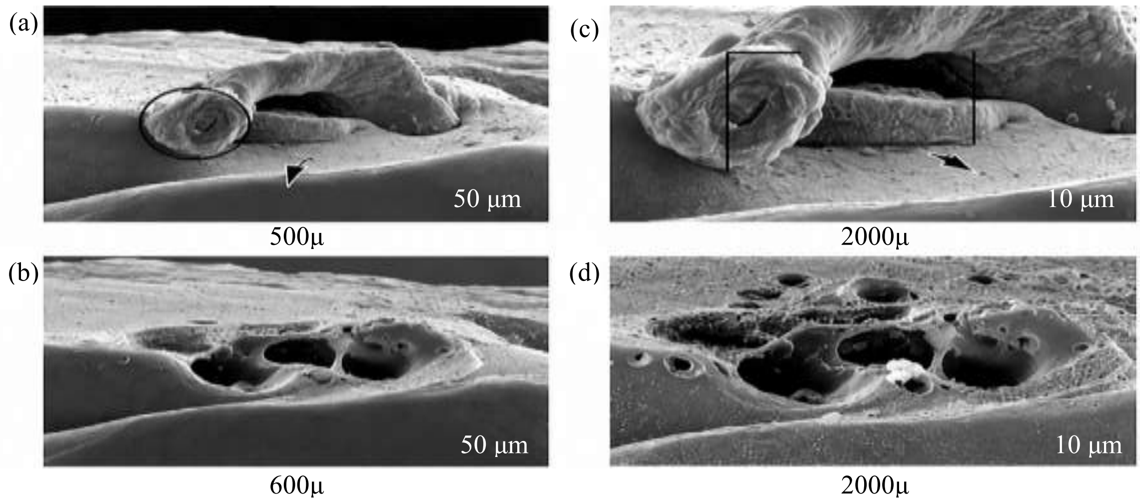

Figure 5. FESEM micrographs of fractured surfaces from tensile tests on basalt-epoxy composites fabricated via VARTM at different fiber volume fractions.

This is corroborated by representative FESEM micrographs at magnifications of 500× and 2000× with scale bars showing excellent interfacial bonding with minimal debonding/pull-out for 50 vol% and increased voids and fiber pull-out for 60 vol%.

The representative photos of fabricated panels, ASTM specimens and post-test fractured samples as shown in Figure 6. Image analysis, by using ImageJ software, in polished cross-sections was cross-validated with the ASTM D2734 method, which is based on the measurement of the density: theoretical and experimental, by using a precision balance, to quantify void fraction. Select samples were also scanned using micro-CT to further validate results.

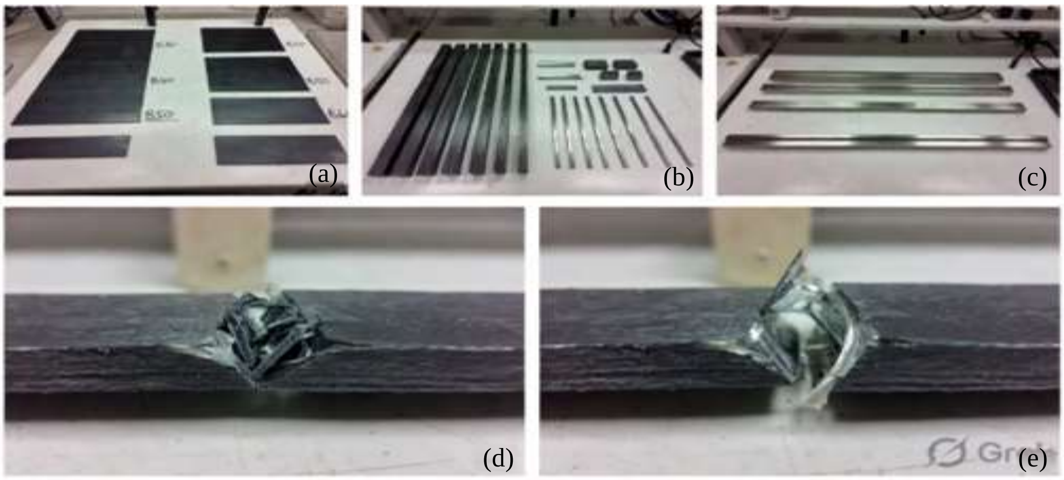

Figure 6. Photographs documenting specimen fabrication, preparation, and failure modes for VARTM basalt-epoxy composites.

Specimen Preparation and Photography

Fabricated laminates, ASTM D638 dog-bone tensile specimens and ASTM D790 flexural specimens were photographed before and after test. The surfaces of the fractures were recorded for the failure mode analysis.

Comparison with Baselines and State-of-the-Art

A detailed comparison of the present VARTM processed basalt/epoxy composites (50 vol% VF) with the earlier baselines and literature is provided in Table 6.

Table 6. Comparison with baselines.

Method	Reinforcement	Tensile strength	Flexural strength	Improvement over glass baseline
Current work (VARTM, 50% Vf)	Basalt	238	295	+22% tensile / +20% flexural
HLC [28]	Basalt	202	–	Baseline
VARIM [29]	Basalt	195	–	+22% (this work)
VBM [30]	Basalt	188	–	+27% (this work)
Literature average (glass-epoxy) [31]	Glass	170–195	220–250	–

The present work also has a higher tensile strength than the hand lay-up with compression moulding (HLC) results obtained from previous studies (202 MPa), which is 18% higher, and the vacuum bagging method (188 MPa), which is 27% higher. The optimized VARTM basalt-epoxy laminates exhibit 15–25% higher tensile and flexural strengths compared to typical literature value for glass-epoxy composite (170–195 MPa tensile) and hand lay-up basalt-epoxy system (180–210 MPa tensile) with a significantly lower void content (<1.5% versus 3–5% for conventional methods). These enhancements corroborate the success of the use of correct VF control and VARTM processing to reduce defects and increase load transfer.

The optimized basalt-epoxy composite (50 vol% VF using VARTM) had higher tensile and flexural strength than the glass-epoxy baseline composite and previously published basalt-epoxy composites produced using the HLC, VARIM and VBM methods as shown in Figure 7.

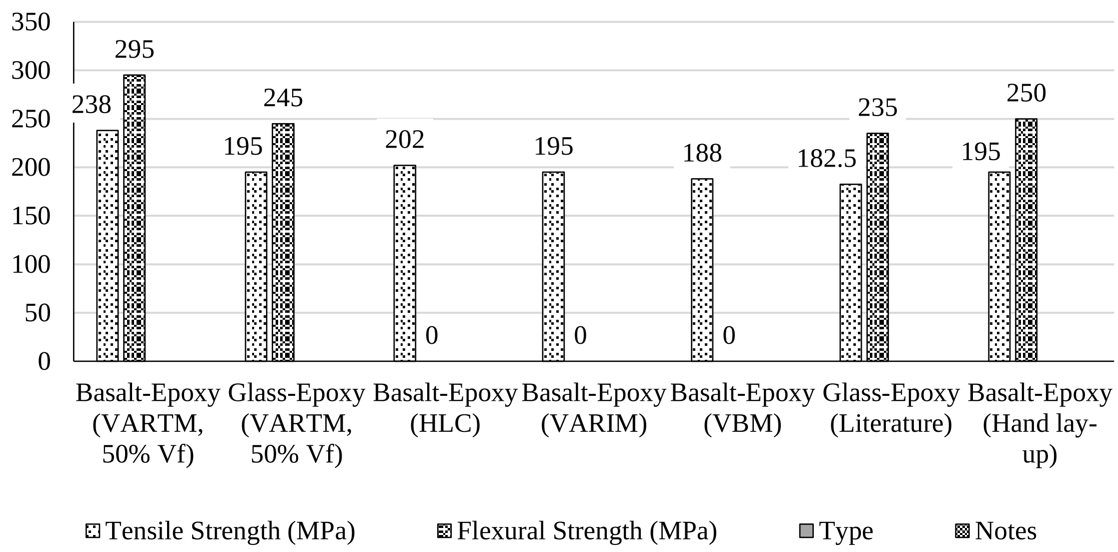

Figure 7. Comparison of tensile and flexural strength of the optimized basalt-epoxy composite with the glass-epoxy baseline and previously reported values from different processing methods.

DISCUSSION

The overall results indicate that the basalt-epoxy composites with VVF of 50 vol% provide the highest tensile strength (238 MPa), flexural strength (295 MPa), and good integrity of the microstructure. The high correlation between the reduction in void content, improvement in fiber–matrix bond and improvement in the mechanical properties further validates the proposed methodology to overcome the major drawbacks of conventional processing methods. The present approach has resulted in these advantages without sacrificing scalability, thus offering clear guidelines to produce high-performance basalt-epoxy laminates for demanding applications in the aerospace, automotive and marine industries.

The results presented fill the identified gaps in research of systematic VF optimization and microstructure-property linkage and provide a basis for the development of multifunctional composites with thermal improvements and structural health monitoring features.

CONCLUSION

This research investigated how the volume fraction of fiber affects tensile and flexural properties of basalt-reinforced epoxy composite made by the VARTM technique The results showed that fiber volume fraction of 50 vol% gave the highest tensile strength (238 MPa) and flexural strength (295 MPa) while the lowest void content (1.1%). The basalt-based composites had always better performance when compared to the glass-based composites with tensile strength approximately 22% and flexural strength approximately 20% higher, respectively. It is believed that this is because of the better fiber–matrix bond and reduced void content in the material produced by the VARTM process the results demonstrate that the proper control of fiber volume fraction along with the use of modern manufacturing processes can lead to the mechanical improvement of sustainable basalt fiber composites. It provides helpful design rules for high strength-low weight composite structures for use in the aerospace, automotive and marine industries. The use of nanofillers in the future can be used and the durability can be tested for a longer period in the environment.

REFERENCES

1. Vyas CJ, Jhala RL. Mechanical characterization of glass-basalt hybrid composites with different fiber weight fraction. Mech Adv Compos Struct. 2024;11(2):295–308. doi: 10.22075/MACS.2024.31330.1541.
2. Reddy SSP, Suresh R, Hanamantraygouda MB, Shivakumar BP. Use of composite materials and hybrid composites in wind turbine blades. Mater Today Proc. 2021;46:2827–2830. doi: 10.1016/J.MATPR.2021.02.745.
3. Hamzat AK, Murad MS, Adediran IA, Asmatulu E, Asmatulu R. Fiber-reinforced composites for aerospace, energy, and marine applications: An insight into failure mechanisms under chemical, thermal, oxidative, and mechanical load conditions. Adv Compos Hybrid Mater. 2025;8(1):152–. doi: 10.1007/S42114-024-01192-Y.
4. Singh SK, Yadav A, Singh S, Jain A, Kumar A. Enhancement of mechanical and viscoelastic properties of epoxy and epoxy–nano silica composites using self-healing microcapsules. Mater Today Commun. 2025;43:111741. doi: 10.1016/J.MTCOMM.2025.111741.
5. da Silva Pinto CE, Arizaga GGC, Wypych F, Ramos LP, Satyanarayana KG. Studies of the effect of molding pressure and incorporation of sugarcane bagasse fibers on the structure and properties of poly (hydroxy butyrate). Compos Part A Appl Sci Manuf. 2009;40(5):573–582. doi: 10.1016/J.COMPOSITESA.2009.02.004.
6. Muhammad JH, Yousif AR. Effect of basalt minibars on the shear strength of BFRP-reinforced high-strength concrete beams. Case Stud Constr Mater. 2023;18:e02020. doi: 10.1016/J.CSCM.2023.E02020.
7. Li S, Yao X, Hou S. Mechanical properties of sustainable fiber-reinforced composites. Acta Mech Sin. 2026;42(2):424874. doi: 10.1007/S10409-025-24874-X.
8. Raajeshkrishna CR, Chandramohan P. Effect of reinforcements and processing method on mechanical properties of glass and basalt epoxy composites. SN Appl Sci. 2020;2(5):959. doi: 10.1007/S42452-020-2774-4.

9. Mani M. Silica nanoparticle-enhanced mechanical properties and energy absorption behavior of hybrid fiber-reinforced polymer composites for structural applications. Next Mater. 2025;9:101213. doi: 10.1016/J.NXMATE.2025.101213.
10. Deng X, Hoo MS, Cheah YW, Tran LQN. Processing and Mechanical Properties of Basalt Fibre-Reinforced Thermoplastic Composites. Polymers (Basel). 2022;14(6). doi: 10.3390/POLYM14061220.
11. Wei ZW, Wang TS, Li HJ, Dong TC, Li Z, Guo X. Study of the flexural behavior of basalt fiber–reinforced concrete beams with basalt fiber-reinforced polymer bars and steel bars. Case Stud Constr Mater. 2025;22:e04433. doi: 10.1016/J.CSCM.2025.E04433.
12. Scalici T, Pitarresi G, Badagliacco D, Fiore V, Valenza A. Mechanical properties of basalt fiber reinforced composites manufactured with different vacuum assisted impregnation techniques. Compos B Eng. 2016;104:35–43. doi: 10.1016/J.COMPOSITESB.2016.08.021.
13. Jia H, et al. Enhanced interfacial and mechanical properties of basalt fiber reinforced poly(aryl ether nitrile ketone) composites by amino-silane coupling agents. Polymer (Guildf). 2021;230:124028. doi: 10.1016/J.POLYMER.2021.124028.
14. Beemkumar N, et al. Thermal stability and flame-retardant properties of a basalt/kevlar fiber-reinforced hybrid polymer composite with bran filler particulates. Results Eng. 2025;25:104207. doi: 10.1016/J.RINENG.2025.104207.
15. Taheri F, Chowdhury SA, Ghiaskar A. Comparison of the Performance of Basalt Fiber-Reinforced Composites Incorporating a Recyclable and a Conventional Epoxy Resin. Polymers. 2025;17(10):1348. doi: 10.3390/POLYM17101348.
16. Mun SY, Ha J, Lee S, Ju Y, Lim HM, Lee D. Prediction of enhanced interfacial bonding strength for basalt fiber/epoxy composites by micromechanical and thermomechanical analyses. Compos Part A Appl Sci Manuf. 2021;142:106208. doi: 10.1016/J.COMPOSITESA.2020.106208.
17. Negru R, Coșa AV, Ianto A, Tătar B, Sîrbu RC, Șerban DA. The Influence of the Manufacturing Technology on the Mechanical Properties of Woven Jute Fiber-Reinforced Epoxy Composites. Polymers. 2025;17(12):1649. doi: 10.3390/POLYM17121649.
18. Gajjar T, Patel P, Joshi S, Shah D. Influence of fiber volume fraction variation on the mechanical properties of CFRP composites manufactured by VARTM process. Next Res. 2025;2(4):100957. doi: 10.1016/J.NEXRES.2025.100957.
19. Debnath S, Maiti S, Adivarekar RV. General testing of wool composites. Wool Fiber Reinforced Polymer Composites. 2022:179–196. doi: 10.1016/B978-0-12-824056-4.00012-1.
20. Mittal V, Saini R, Sinha S. Natural fiber-mediated epoxy composites – A review. Compos B Eng. 2016;99:425–435. doi: 10.1016/J.COMPOSITESB.2016.06.051.
21. Yang X, Zhan L, Peng Y, Liu C, Xiong R. Interface Controlled Micro- and Macro-Mechanical Properties of Vibration Processed Carbon Fiber/Epoxy Composites. Polymers. 2021;13(16):2764. doi: 10.3390/POLYM13162764.
22. Tian Y, Zhang H, Zhang Z. Influence of nanoparticles on the interfacial properties of fiber-reinforced-epoxy composites. Compos Part A Appl Sci Manuf. 2017;98:1–8. doi: 10.1016/J.COMPOSITESA.2017.03.007.
23. Kim JH, et al. Interfacial properties and permeability of three patterned glass fiber/epoxy composites by VARTM. Compos B Eng. 2018;148:61–67. doi: 10.1016/J.COMPOSITESB.2018.04.041.
24. Musa AA, Park J, Hong G, Yoon SH, Onwualu AP, Kim M. Development of high-performance basalt fiber–reinforced polymer composite using a nanocellulose-based surface modification strategy. Compos Part A Appl Sci Manuf. 2025;199. doi: 10.1016/J.COMPOSITESA.2025.109191.
25. Rahman MM, Ismail AE, Ramli MF, Rashid AHA. Predicting flexural properties of fiber reinforced composites: An experimental dataset analysis using machine learning models. Next Mater. 2026;11:101720. doi: 10.1016/J.NXMATE.2026.101720.
26. Farsani RE, Daghigh V, Derakhshani K. Tensile and flexural properties of basalt fibers/nano-alumina powder-reinforced multi-scale composites. Surfaces Interfaces. 2024;46:104009. doi: 10.1016/J.SURFIN.2024.104009.
27. Subagia A, Kim YJ. Influence of volume fraction of basalt fabrics on tensile and three-point bending behaviours of hybrid composites reinforced with carbon/basalt fabrics. AIP Conf Proc. 2023;2568. doi: 10.1063/5.0114190.

28. Wang Y, et al. Quasi-static and high-rate flexural responses of intralaminar-hybridised basalt-flax fibre-reinforced polymer composites. Adv Compos Hybrid Mater. 2025;9(1):26–. doi: 10.1007/S42114-025-01559-9.
29. Chowdhury IR, O'Dowd NP, Comer AJ. Experimental study of hygrothermal ageing effects on failure modes of non-crimp basalt fibre-reinforced epoxy composite. Compos Struct. 2021;275:114415. doi: 10.1016/J.COMPSTRUCT.2021.114415.
30. Bulut M. Mechanical characterization of Basalt/epoxy composite laminates containing graphene nanopellets. Compos B Eng. 2017;122:71–78. doi: 10.1016/J.COMPOSITESB.2017.04.013.
31. Rajkumar DR, et al. Mechanical and environmental performance of laminated composite plates reinforced with natural and synthetic fibers: A comparative study of flexural, water absorption and swelling characteristics. Discover Sustainability. 2025;6(1):905–. doi: 10.1007/S43621-025-01550-W.

